Rock Mechanics and Rock Engineering (2023) 56:6855–6877
https://doi.org/10.1007/s00603-023-03429-6

ORIGINAL PAPER

Spatial–Temporal Evolution and Countermeasures for Coal and Gas Outbursts Represented as a Dynamic System

Chaojun Fan[1,2] · Lingjin Xu[2] · Derek Elsworth[3] · Mingkun Luo[4] · Ting Liu[5] · Sheng Li[2] · Lijun Zhou[2] · Weiwei Su[1]

Received: 29 March 2023 / Accepted: 15 June 2023 / Published online: 1 July 2023

Abstract

The occurrence of dangerous coal and gas outbursts seriously threaten safety in underground coal mining. Thus, defining the spatio-temporal evolution of the mechanisms that contribute to these outbursts is of great significance in defining optimal countermeasures for outburst prevention. A dynamic system-based mechanism of coal and gas outbursts is proposed to define conditions that define the formation and instability criteria of outburst dynamics. A stress–damage–seepage coupled model is devised to represent gassy outbursts from the coal seam that couples elastic-damage and permeability evolution. Numerical solution of this coupling model is used to investigate the spatio-temporal evolution of coal and gas outbursts. The spatial scales of both the outburst system and the geological body are discussed, as well as countermeasures for prevention. We show that the outburst dynamic system comprises a gassy coal mass combined with a geo-dynamic environment and mining disturbance. The evolution through failure involves stages of *initialization*, *formation*, *development* then *termination*. The dynamic system forms when the mining damage zone and the tectonic damage zone coalesce. Stress transfer, gas migration, energy accumulation then release in the dynamic system are shown as key contributing features to the dynamic outburst, as well as the three-dimensional structure of the dynamic system and geological body. A released energy density greater than the required dissipation energy density is the key to determine whether an outburst can continue. This criterion defines countermeasures for outburst prevention that include unloading and depressurization, which either reduce the geo-stress or the gas pressure and content in the coal seam to avoid the instability criterion for the formation of the dynamic system.

Highlights

- A stress-damage-seepage coupled model is derived to represent coal and gas outbursts.
- The spatio-temporal evolution of coal and gas outbursts is investigated.
- An energy based instability criteria is proposed to determine whether an outburst can continue.
- Countermeasures for outburst prevention include unloading and depressurization.

Keywords Coal and gas outburst · Spatial–temporal evolution · Countermeasures · Multi-physics coupling · Dynamic system · Damage zone · Spatial scale

✉ Chaojun Fan
chaojunfan@139.com

[1] State Key Laboratory of Coal Mine Safety Technology, China Coal Technology & Engineering Group Shenyang Research Institute, Shenyang 113122, China

[2] College of Mining, Liaoning Technical University, Fuxin 123000, China

[3] Energy and Mineral Engineering, The Pennsylvania State University, University Park, PA 16802, USA

[4] Energy Business Department, Shanxi Lu'an Chemical Group, Changzhi 046200, China

[5] School of Safety Engineering, China University of Mining and Technology, Xuzhou 221116, China

1 Introduction

Coal and gas outbursts comprise a complex dynamic process that may occur during underground coal production (Tian et al. 2021; Zhou et al. 2021a). A large mass of coal and gas is ejected from the coal mass into the mining space, damaging roadways or the working face (Rudakov and Sobolev 2019; Kong et al. 2022). The demand for coal resources in China continues to increase, resulting in a necessary increase in depth and intensity of coal mining. Concurrent with this increase in depth, stresses and gas pressures increase, with the intensity and frequency of coal and gas outburst disasters increasing (Zhang et al. 2018; Li et al. 2021). In October 2010, a gas outburst occurred in the Pingyu No.4 Coal Mine of the Henan Pingmei Group, China, resulting in 37 deaths (Yuan 2016). The combined action of stress and gas pressure is implicated in the outburst although the exact mechanisms remain unclear (Wang and Cheng 2023). To clarify mechanisms, we examine the dynamic failure of gassy coal from the viewpoint of energy dissipation in the outburst process and accommodating the multi-physics of the coupling (Liu et al. 2021).

Outburst mechanisms are divided into two categories: single-factor and multi-factor mechanisms (Ma et al. 2020). The multi-factor mechanism is widely accepted, but all statistical phenomena during a single outburst cannot be explained using present knowledge. Additional topics about outburst mechanisms are proposed by summarizing the phenomena that need precise explanation. The evolution through triggering then generation of coal and gas outbursts have been studied through field observation, physical and theoretical analysis, and numerical simulation (Fan et al. 2017). Mechanistic hypotheses involving various interactions of gas overpressures, the dominance of stresses, chemical effects have been advanced to qualitatively explain coal and gas outbursts (Zhou et al. 2021a; Xue et al. 2023; Guo et al. 2023). In terms of a comprehensive hypothesis, coal and gas outbursts have been considered as a mechanical failure process where the coal and rock system is dynamically destabilized by external agents (Zhang et al. 1991; Soleimani et al. 2023). The outburst process may be divided into several stages (Shu et al. 2023a; Hu et al. 2008) and various criteria for initiation defined (Shu et al. 2017).

Fluid–solid coupling is a leading contender to codify the spectrum of mechanisms observed to act at various length and time scales (Liang 2000; Wang et al. 2022). Incorporating the effects of gas pressures and compressibility, stress, coal mechanical properties, energy accumulation and release during the instability of an outburst, the gas seepage–stress–damage coupling model in mining disturbed coal and rock mass is a popular rationalization that accommodates most observed phenomena (Xu et al. 2006; Liu et al. 2016). Based on the multi-scale structural characteristics and spatial–temporal variability of coal, the fluid–solid coupling behavior in multi-scale fractured coal is accommodated in three aspects—the interaction between the coal matrix and fractures, the mechanical properties of gas-bearing coal with multi-phase coupling in the pores and the evolution of damage during seepage coupling within the coal seam (Hu 2015; Xu et al. 2019). Coal seams are typically characterized as a dual porosity medium (Shu et al. 2022; An et al. 2013). The influence of seepage and desorption processes on the initial conditions of coal and gas outbursts was discussed (Sobczyk 2014).

Various models have enabled the energetic state and evolution of the dissipation of energy within the coal and gas to be followed with the progress of the outburst (Tang et al. 2000; Xiong et al. 2015), as well as characterizing mechanisms of energy dissipation (Wang et al. 2015a, 2015b; Shu et al. 2023b) The energy-limiting factor was proposed for coal and gas outburst occurrence in intact coal seam, and the needed strain energy accompanying with the required minimum stress for the crushing work was estimated (Shu et al. 2023b; Tu et al. 2021). Recently, scholars considered the response characteristics of gas pressure under simultaneous static and dynamic load, assuming that coal and gas outburst is a high-speed loading environment with two-phase gas–solid outbursts in roadways (Zhang et al. 2021; Zhou et al. 2021b).

The above research only studied the interaction between coal and gas, or the energy release from coal rock fracture and gas, or the dynamic process, but failed to systematically integrate these ideas to elaborate on the occurrence mechanism of coal and gas outburst from the mathematics to spatial–temporal evolution and countermeasures. We follow the evolution of coal and gas outbursts as a dynamic system by defining an instability criterion. We consider the evolution of permeability in an elastic coal mass undergoing damage, as a problem in stress–damage–seepage coupling. We define the governing equations defining the stress field and gas transport from desorption and diffusion from the matrix to the embedded fractures. This model enables the roles of stress transfer, gas migration, energy accumulation then release to be incorporated into the run-up to the outburst. The model enables the key features contributing to the outburst to be determined and methods for their mitigation defined.

2 Mechanism of Coal and Gas Outburst Based on Dynamic System

Coal and gas outbursts comprise three mandatory components: a gassy coal seam, a stressed environment, and mining disturbance. The gassy coal seam and stressed environment

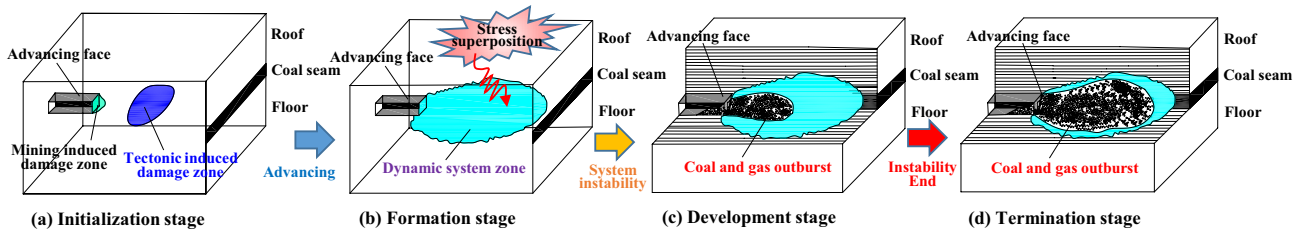

Fig. 1 Evolution of a coal and gas outburst

result from tectonic evolution. Mining disturbance drives damage, then failure of the coal–rock system in the early stage of the outburst, and provides the conditions for rapid release of gas and coal as an instability comprising the outburst (Fan et al. 2017). The outburst experiences the four stages of initialization, formation, development, and termination, as shown in Fig. 1.

At *initialization*, the system is primed by tectonic movement, then disturbed through engineering activities that alter the physical and mechanical properties of the coal seam. A tectonically induced damage zone results, which produces the stress state and gas accumulation conditions conducive to the outburst. As the roadway is excavated, the stress balance is disturbed and a mining-induced damage zone is generated ahead of the advancing face.

In the *formation stage*, a large damage zone evolves around the roadway under the combination of tectonic and mining stresses (Guo et al. 2016a). When the roadway advances close to this zone of tectonically induced damage, the stress redistribution within surrounding rock caused by mining, blasting, mechanical vibration, gravity and tectonic movement, is dynamically superimposed. Under the action of compressive stress, the bedding fractures parallel to the roadway axis in the damage area are closed, hindering the migration of gas to the roadway space. Simultaneously, massive fractures perpendicular to the axis of the roadway are developed, which promote the desorption of adsorbed gas and production of free gas at high pressure in the fractures. The outburst initiates by comminuting the coal seam to particles and shortens the path of gas desorption and migration to individual fractures. As a result, the gas desorption time is sharply decreased, and the desorbed gas will rapidly sublimate in the outburst process. The coal outside the damage zone remains elastic and with native low permeability, in which the gas migration is impeded and with failure of the coal participates in the outburst.

In the *development stage*, the coal mass in the damage zone near the advancing face undergoes tensile failure, and becomes unstable. The unstable and broken gassy coal mass is ejected as a mixture of gas and coal particles with high kinetic energy. The high-pressure gas expands to propel the coal–rock–gas mixture forward, resulting in the formation of a remnant cavity. Gas desorbs rapidly from the coal wall and migrates into the roadway. The coal face continues to undergo tensile failure and is thrown out under the ground stresses and gas pressure gradient with the cavity deepening. The outburst may pause as the coal face is temporarily unable to meet the instability criterion. At this time, the coal face continues to undergo quasi-static deformation and failure, and releases gas into the outburst cavity, resulting in a sharp increase of the gas pressure gradient around the free space. If the gas pressure gradient reaches a threshold value, the accumulating crushed coal will be thrown out again.

In the *termination stage*, when the pressure gradient caused by the gas accumulation in the cavity is unable to further eject the coal–rock–gas mixture, the wall of the cavity will stabilize, and the coal and gas outburst terminates. It is necessary to note that the tectonic damage zone ahead of the advancing face may be caused by the dynamic environment pre-mining in the *initialization* or *formation stages*, or by the combined effect of the mining disturbance and the dynamic environment following the initiation of mining. In extreme cases, the outburst may also be caused by the mining disturbance alone, without the formation of the tectonic damage zone. In addition, the suspension and restart of coal and gas outbursts in the *development stage* are not inevitable, as the conditions after restart following suspension may not be meet, and finally the gas outburst is terminated.

3 Formation and Instability Criterion for Gas Outbursts

3.1 Forming Criterion

The priming of the coal–rock mass ahead of the advancing face is the premise for the occurrence of an outburst. As shown in Fig. 2, the low-strength coal–rock mass in the tectonic damage zone is acted on by the tectonic stress. When the advancing face advances to adjacent to the tectonic damage zone, the minin- induced stress and the tectonic stress around the tectonic zone are superimposed to generate an instantaneous load. This acts on the coal–rock mass around

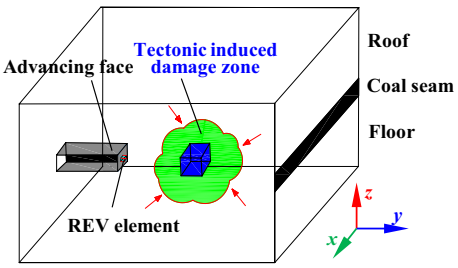

Fig. 2 Spatial relationships between zones adjacent to the advancing face

the tectonic zone and the location between the tectonic zone and the advancing face.

The maximum tensile stress criterion and Mohr–Coulomb criterion are used to determine whether tensile or shear damage occurs after the coal is stressed. The formation criterion of the unstable system can be expressed as (Chen et al. 2018):

$$F_1 = \begin{cases} \sigma_1 - \sigma_t \geq 0 \\ -\sigma_3 + \sigma_1 \dfrac{1+\sin\theta}{1-\sin\theta} - \sigma_c \geq 0 \end{cases} \tag{1}$$

where σ_1 is the maximum principal stress, Pa; σ_3 is the minimum principal stress, Pa; σ_t and σ_c are tensile and compressive strength of the coal respectively, Pa; θ is the internal friction angle of the coal, and; F_1 is the threshold functions for tensile or shear damage. The positive sign means tension, while the negative sign means compression.

3.2 Instability Criterion

The maximum tensile strength criterion and the Mohr–Coulomb criterion can be used to determine whether the representative element volume (REV) is damaged – this criterion will condition the location or scale of the outburst region. However, damage to the REV does not necessarily result in instability of the coal mass. An instability criterion for the system will be established based on energy conservation. The actions of the internal energy of the gas, the elastic potential energy, and gravitational potential energy conspire to fracture the coal. The internal and potential energies will contribute to the crushing work and the kinetic work of the fragmented coal. Ignoring the energy dissipated by frictional heating, vibration and sound, the instability process must satisfy (Hu et al. 2008):

$$E_g + E_p + E_e \geq E_k + E_f \tag{2}$$

where E_g is the internal energy of the outburst gas, J/m^3; E_p is the gravitational potential energy of the outburst coal–rock mass, J/m^3; E_e is the elastic potential energy of the outburst coal mass, J/m^3; E_f is the crushing work required for the coal–rock mass in the dynamic system, J/m^3; E_k is the kinetic work required for the outburst coal, J/m^3.

Gas is transported into the roadway from the coal mass and gas pressure will decrease from p_1 to p_2 resulting in the released gas internal energy as (Wang et al. 2015b):

$$E_g = \left(\frac{\varphi s_g p_1 T_0}{T p_0 \rho_s} + \frac{\eta V_L p_1}{P_L + p_1}\right) \frac{\rho_s p_1}{n-1} \left[\left(\frac{p_1}{p_2}\right)^{\frac{n-1}{n}} - 1\right] \tag{3}$$

where φ is the porosity of coal; η is the proportion of adsorbed gas participating in the outburst in total adsorbed gas, which is related to the initial velocity of diffusion; n is the process index, and the adiabatic process can be taken as 1.25; ρ_s is the density of the coal mass, kg/m^3; V_L is Langmuir volume constant, m^3/kg; P_L is Langmuir pressure constant, Pa; s_g is gas saturation in the fractures; T_0 is the standard temperature, K, and; p_0 is standard atmospheric pressure, Pa.

The gravitational potential energy of coal–rock mass is expressed as:

$$E_p = \rho_s g h \tag{4}$$

where g is the acceleration due to gravity, m/s^2; h is the relative height between the pre-outburst and post-outburst positions of the coal–rock, m.

The elastic potential energy of the coal–rock mass is expressed as:

$$E_e = \frac{1}{2E}\left[\sigma_1^2 + \sigma_2^2 + \sigma_3^2 - 2\mu\left(\sigma_1\sigma_2 + \sigma_2\sigma_3 + \sigma_1\sigma_3\right)\right] \tag{5}$$

where σ_1, σ_2, and σ_3 are the maximum, intermediate, and minimum principal stresses on the coal, MPa.

The crushing work required for the coal–rock mass is (Hu et al. 2008):

$$E_f = C f^A Y_{p1}^B \rho_s \tag{6}$$

where Y_{p1} is the percentage of the mass of coal broken into particle sizes < 0.2 mm in the total coal mass; f is the firmness coefficient of the coal in the dynamic system; A, B, C are fitting coefficients. By fitted with results of impact crushing tests on 21 coal samples from outburst Coal Mine in China, the coefficients A, B, C are determined as 46.914 J/kg, 1.437, and 1.679.

The kinetic work required for the outburst is (Wang et al. 2015a):

$$E_k = \frac{\rho_s v^2}{2} \tag{7}$$

where v is the transport speed of the coal mass, m/s.

Substituting Eqs. (3–7) into Eq. (2), the instability criterion for the dynamic system can be obtained:

$$F_2 = \left(\frac{\varphi s_g p_1 T_0}{T p_0 \rho_s} + \frac{\eta V_L p_1}{P_L + p_1}\right)\frac{\rho_s p_1}{n-1}\left[\left(\frac{p_1}{p_2}\right)^{\frac{n-1}{n}} - 1\right] + \rho_s g h + \frac{\sigma_1^2 + \sigma_2^2 + \sigma_3^2 - 2\mu\left(\sigma_1\sigma_2 + \sigma_2\sigma_3 + \sigma_1\sigma_3\right)}{2E} - Cf^A Y_{p1}^B \rho_s - \frac{\rho_s v^2}{2} \geq 0 \tag{8}$$

The instability criterion of the dynamic system involves the regional tectonic stress, mining-induced stress, strength of the coal–rock mass and gas properties. These parameters reflect the interactions among the coal–rock mass, geo-stress, gas and conforms to conservation of energy. The occurrence of coal and gas outbursts require that both the formation criterion and the instability criterion are satisfied.

4 Stress–Damage–Seepage Coupling Model for Outbursts in Coal Seams

4.1 Basic Assumptions

Coal and gas outbursts involve an instability in coal deformation–failure and gas rapid desorption–diffusion–seepage. In this section, we develop the stress–damage–seepage coupling model for outbursts in coal seams and a method for numerical simulation. The coal is characterized as a pore-fracture dual porosity structure with the coal composed of coal matrix (containing micro-pores) and fractures. To simplify the complex processes of outburst evolution, the following basic assumptions are made:

- The fracture network transects and is embedded within the coal matrix. Gas and water are present in the coal matrix and is also the main medium for mass transfer. Because the matrix permeability is very low, only the fracture permeability is considered.
- The coal matrix comprises the coal skeleton and micro-pores. The inner surface of the micro-pores can adsorb a large amount of gas; meantime free gas exists in the micro-pore space.
- Groundwater exists and migrates only in fractures. The fractures are saturated by water and gas.
- Gas desorption from the inner surface of the micro-pores in coal matrix follows the Langmuir adsorption isotherm and the gas adsorption/desorption process evolves instantaneously.
- The gas diffuses from the matrix pore to the fractures under the action of the concentration gradient, governed by Fick's first law.
- Gas seepage from the fracture to the roadway follows Darcy's law.
- The migration of gas and water in the coal seam evolves isothermally.
- The gas is regarded as ideal and the seepage and gravity force of gas is ignored.
- The tensile stress is positive and compressive stress is negative.
- Coal and gas outburst is a high-speed loading environment that the strain rate effects may be obvious (Lu et al. 2017). However, we did not consider the strain rate effect in the strength of the material in the model because of the great time consumption and difficulty in calculation in this study.

4.2 Governing Equations

The total strain of the coal includes strain caused by solid stress, by fluid pressure in the pores and fissures, and by gas adsorption/desorption. The governing equation of the stress field can be expressed as a modified Navier equation (Li et al. 2016):

$$Gu_{i,jj} + \frac{G}{1-2\upsilon}u_{j,ji} - \left(\frac{K}{K_m} - \frac{K}{K_s}\right)p_{m,i} - \left(1 - \frac{K}{K_m}\right)p_{f,i} - K\left(\frac{\varepsilon_{\max} p_m}{P_s + p_m}\right)_{,i} + F_i = 0 \tag{9}$$

where G is the shear modulus of coal, Pa; K is the bulk modulus of coal, $K = E/3(1-2\nu)$, Pa; α_m and α_f are Biot's effective stress coefficients corresponding to pores and fractures respectively; p_m is the pressure in matrix pores, MPa; p_f is the fluid pressure in the fractures, Pa; E is the elastic modulus of the coal, Pa; υ is Poisson's ratio; K_m is the elastic modulus of the coal matrix, $K_m = E_m/3(1-2\nu)$, Pa; E_m is the bulk modulus of the coal matrix, Pa; K_s is the bulk modulus of the coal skeleton, Pa; Ps is the Langmuir-type stress coefficient, Pa; $\varepsilon_{\max}$ is the maximum strain of coal.

Stress concentrations develop ahead of the advancing face, and this damages the coal seam. The elastic modulus of the coal decreases with the damage and may be expressed as (Fan et al. 2017):

$$E = E_0(1 - D) \tag{10}$$

where E and E_0 are the elastic modulus of coal post- and pre-damage, respectively, Pa; D is the damage variable.

The maximum tensile stress criterion and the Mohr–Coulomb criterion are used to determine whether tensile and shear damage occur in the coal seam. The damage variable in coal is expressed as (Xu et al. 2006):

$$D=\begin{cases}0 f_1<0, f_2<0\\ 1-\left(\dfrac{\varepsilon_{t0}}{\varepsilon_t}\right)^2 f_1=0, df_1>0\\ 1-\left(\dfrac{\varepsilon_{c0}}{\varepsilon_c}\right)^2 f_2=0, df_2>0\end{cases} \tag{11}$$

where $f_1=\sigma_1-\sigma_t$, $f_2=-\sigma_3+\sigma_1\frac{1+\sin\theta}{1-\sin\theta}-\sigma_c$; ε_t is the maximum tensile strain in the coal; ε_c is the minimum compressive strain in the coal; ε_{t0} represents the ultimate tensile strain in the coal; ε_{c0} represents the ultimate compressive strain in the coal. The calculation details of the damage variable are shown in Fig. 3.

The governing equation for gas migration in the coal matrix is:

$$\frac{\partial}{\partial t}\left(\frac{V_L p_m}{P_L+p_m}\rho_s\rho_{gs}+\varphi_m\frac{M_g p_m}{RT}\right)=-\frac{M_g\left(p_m-p_{fg}\right)}{\tau RT}e^{\alpha_{D1}D} \tag{12}$$

where φ_m is the porosity in coal matrix; M_g is the molar mass of gas, kg/mol; R is the molar constant of gas, J/(mol·K); T is the temperature in the coal seam, K; V_L is Langmuir volume constant, m^3/kg; P_L is the Langmuir pressure constant, Pa; ρ_{gs} is gas density in standard state, kg/m^3; α_{D1} is the coefficient of damage on desorption rate; τ is the gas desorption time, s.

Combined with the generalized Darcy's law for two-phase gas–water seepage, the mass conservation equation of the gas phase in the fracture system can be expressed as (Wu et al. 2010; Pan and Connell 2012):

$$\begin{aligned}&\frac{\partial\left(s_g\varphi_f\rho_g\right)}{\partial t}+\nabla\cdot\left(-\rho_g\frac{kk_{rg}}{\mu_g}\left(1+\frac{b_k}{p_{fg}}\right)\nabla p_{fg}\right)\\&=\left(1-\varphi_f\right)\frac{M_g\left(p_m-p_{fg}\right)}{\tau RT}e^{\alpha_{D1}D}\end{aligned} \tag{13}$$

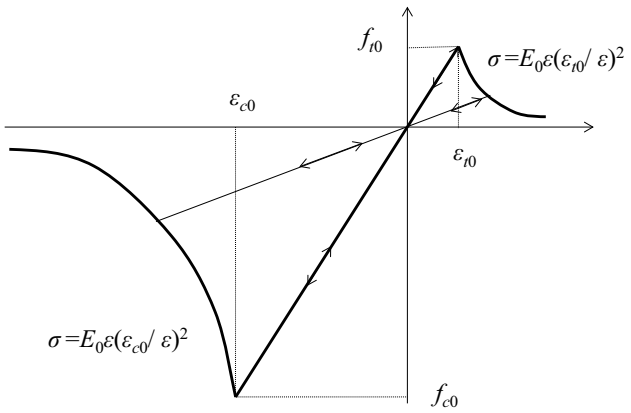

Fig. 3 Stress–strain curve of coal seam post- and pre-damage

where φ_f is the fracture porosity; k is the absolute fracture permeability, m^2; k_{rg} is the relative permeability of gas; μ_g is dynamic viscosity of CH_4, Pa·s; b_k is the slippage factor, Pa.

The mass conservation equation for the water phase in fracture system can be expressed as:

$$\frac{\partial\left(s_w\varphi_f\rho_w\right)}{\partial t}+\nabla\cdot\left(-\rho_w\frac{kk_{rw}}{\mu_w}\nabla p_{fw}\right)=0 \tag{14}$$

where ρ_w is the water density, kg/m^3; k_{rw} is the relative permeability to water; μ_w is the dynamic viscosity of water, Pa·s.

Based on the capillary pressure curve, Corey proposed the relative permeability model of gas–water two-phase flow, which was later confirmed to accurately reflect the migration law of water and gas in coal seams. The model is (Fan et al. 2019):

$$\begin{cases}k_{rg}=k_{rg0}\left(1-\left(\dfrac{s_w-s_{wr}}{1-s_{wr}-s_{gr}}\right)\right)^2\left(1-\left(\dfrac{s_w-s_{wr}}{1-s_{wr}}\right)^2\right)\\ k_{rw}=k_{rw0}\left(\dfrac{s_w-s_{wr}}{1-s_{wr}}\right)^4\end{cases} \tag{15}$$

where s_{wr} is the bound water saturation; s_{gr} is residual gas saturation; k_{rg0} is the gas phase endpoint relative permeability; k_{rw0} is the relative permeability of the water phase endpoint.

The coal seam is initially in a state of elastic deformation. After disturbance by mining or excavation, the stress state ahead of the advancing face changes, and the coal is damaged or fails. The loading and unloading effect on the coal ahead of the advancing face triggers the original fractures to expand, generates new fractures that then extend and penetrate, with the coal matrix also damaged or failed. The development and penetration of fractures in the coal promote the rapid migration of gas and water. The damage-induced permeability of the coal increases rapidly, which may reach 300–500 times that of the initial state (Guo 2017). Therefore, the permeability of coal ahead of the advancing face is divided into elastically influenced permeability and damage-influenced permeability.

The evolution of coal permeability is related to the change in fracture opening and fracture volume in coal. In the elastic stage, the change in fracture volume results from the effective stress-induced strain and the gas adsorption-induced strain. According to previous studies, the porosity in the coal matrix can be expressed as (Fan et al. 2019):

$$\phi_m = \phi_{m0} + \frac{(\alpha_m - \phi_{m0})(\varepsilon_e - \varepsilon_{e0})}{(1+\varepsilon_e)} \tag{16}$$

where $\varepsilon_e = \varepsilon_v + p_{mg}/K_s - \varepsilon_s$; ε_v is the volumetric strain of the coal; the subscript '0' represents the initial value.

The fracture state in the coal can be defined as:

$$\phi_f = \frac{3b_0(1+\Delta\varepsilon_f)}{a} \tag{17}$$

and the relationship between permeability and fracture porosity satisfies the cubic law, and the permeability can be obtained as:

$$\frac{k}{k_0} = \left[1 + \frac{3(1-R_m)}{\phi_{f0}}\left(\Delta\varepsilon_{ti} - \frac{1}{3}f_m\Delta\varepsilon_s\right)\right]^3 \tag{18}$$

Considering the anisotropy in permeability, the coal permeability in the different coordinate directions (k_x, k_y, k_z) under the elastic state is given as:

$$\frac{k_{ei}}{k_{i0}} = \sum_{i\neq j}\frac{1}{2}\left[1 + \frac{3(1-R_m)}{\phi_{f0}}\left(\Delta\varepsilon_{tj} - \frac{1}{3}f_m\Delta\varepsilon_s\right)\right]^3 \tag{19}$$

where k_{i0} is the initial permeability in the i direction, m^2.

If the coal seam is damaged, the permeability is mainly controlled by the evolution of damage and fracture creation. The sudden increase coefficient ζ is introduced into the coal permeability model to represent the abrupt change in permeability caused by the damage (Cui and Bustin 2005; Zheng et al. 2017). The sudden increase coefficient increases exponentially with the damage variable, which can be expressed as (Xue et al. 2015):

$$\xi = e^{\alpha_D D} \tag{20}$$

where α_D is the damage coefficient; and D is the damage variable.

Considering the pore pressure and damage evolution, the damage-based permeability model for the coal is (Xue et al. 2015):

$$k_{di} = k_{i0}\sum_{i\neq j}\frac{1}{2}\left[1 + \frac{3(1-R_m)}{\phi_{f0}}\left(\Delta\varepsilon_{tj} - \frac{1}{3}f_m\Delta\varepsilon_s\right)\right]^3 e^{\alpha_D D} \tag{21}$$

According to Eq. (19) and Eq. (21), the permeability model for the evolution of coal from elastic to damaged state is obtained as:

$$\begin{cases} k_i = k_{i0}\sum_{i\neq j}\frac{1}{2}\left[1 + \frac{3(1-R_m)}{\phi_{f0}}\left(\Delta\varepsilon_{tj} - \frac{1}{3}f_m\Delta\varepsilon_s\right)\right]^3, F_1 < 0, F_2 < 0 \\ k_i = k_{i0}\sum_{i\neq j}\frac{1}{2}\left[1 + \frac{3(1-R_m)}{\phi_{f0}}\left(\Delta\varepsilon_{tj} - \frac{1}{3}f_m\Delta\varepsilon_s\right)\right]^3 e^{\alpha_D\left[1-(\varepsilon_{t0}/\varepsilon_t)^2\right]}, F_1 = 0, dF_1 > 0 \\ k_i = k_{i0}\sum_{i\neq j}\frac{1}{2}\left[1 + \frac{3(1-R_m)}{\phi_{f0}}\left(\Delta\varepsilon_{tj} - \frac{1}{3}f_m\Delta\varepsilon_s\right)\right]^3 e^{\alpha_D\left[1-(\varepsilon_{c0}/\varepsilon_c)^2\right]}, F_2 = 0, dF_2 > 0 \end{cases} \tag{22}$$

Combining Eqs. (9–22), the stress–damage–seepage coupling model for coal containing gas is obtained, and the full coupling among key physical fields of stress, damage, diffusion, and seepage in coal containing gas is defined. The stress–damage–seepage coupling model for coal containing gas is composed of several complex second-order partial differential equations (PDEs). Due to their time–space nonlinearity, it is difficult to solve these by analytical methods (Wu et al. 2010). Hence, the finite element method (FE) is used for numerical solution.

4.3 Solving Method for Stress–Damage–Seepage Coupling Model

There are some advanced numerical algorithms, such as the robust stress update algorithm for elastoplastic models without analytical derivation of the consistent tangent operator and loading/unloading estimation, the

open-source unconstrained stress updating algorithm for the modified Cam-clay model, et al. (Lu et al. 2023; Zhou et al. 2022). Here, we solve the proposed model using the scripts linking Comsol with Matlab to codify the stress–damage–seepage coupled model. The solid mechanics module is used to calculate the stress evolution during the outburst, and the PDE modules are used to evaluate gas desorption, diffusion, and gas–water two-phase seepage migration during the outburst. Coal damage is concurrently evaluated. The damage variable and permeability are defined in Matlab scripts and their values are linked to Comsol for the spatial evaluation of the PDEs. Fracture development and propagation and rapid gas desorption and seepage in the dynamic process are followed.

The evolution of damage and gas and water migration in the coal seam are all followed in time, and a transient solution is adopted. The load on the coal gradually increases and is regarded as a quasi-static process as the fields of stress, damage, and seepage in the coal stabilize over a very short time increment Δt_i at time t_i. For the simulation of the compressive seepage process in the coal, the sample is gradually loaded from zero to the target load. The procedures of loading are listed as follows:

- Step 1: Initialize the Comsol with Matlab routines, build the geometric model, establish the solid mechanics module, and initiate the PDE modules for the equations of gas desorption, diffusion, and seepage, and water seepage.
- Step 2: Evaluate the heterogeneous elastic modulus of the coal, input the initial value of the parameters, set the boundary conditions for the solid and fluid, and mesh of geometric model.
- Step 3: Apply the first stress loading, and solve for the variables, *i.e.,* stress, strain, damage, gas pressure and water saturation.
- Step 4: Extract the effective stresses and strains to obtain the distribution of the damage variables, and evaluate the stress state of element and whether it meets the criterion for the occurrence of new damage. If there is new damage, the parameters, including elastic modulus, strength and permeability of coal are modified. Adjust the stress within the coal accordingly, and complete successive cycle of calculation until no new damage occurs.
- Step 5: Increment of the solution step, apply the next loading, continue to steps 3 and 4, and repeat until the target load is achieved.
- Step 6: Conduct post-processing, and terminate the Comsol with Matlab routines.

5 Modeling the Spatio-temporal Evolution of the Outburst

5.1 Geometry and Settings

We follow the evolution of a serious coal and gas outburst that occurred on October 20, 2004 in the Daping Coal Mine, of the Zhengzhou Coal Group, China. A gas explosion resulted in 148 deaths and 32 injuries (Guo et al. 2016a). The roadway encountered a squeezing reverse fault with a vertical offset of ~ 10 m during the excavation process. A coal and gas outburst occurred when the coal seam on the underside of the reverse fault was excavated. The outburst was of 1894 t of coal–rock (1362 t of coal and 532 t of rock) and 250,000 m^3 of outburst gas. As shown in Fig. 4a, the outburst face of the excavating roadway is ~ 5 m from the coal seam on the underside of the reverse fault. The buried depth of the coal seam is 612 m. The outburst cavity is located in the middle and upper parts of the advancing face. The opening of the cavity is 2.2 m in width, 1.6 m in height, and 7.3 m in length. The upward inclination angle of the cavity is 43°, which is coincident with the orientation of the fault surface (Luo et al. 2018).

As shown in Fig. 4b, a three-dimensional geometric model reflecting the outburst in situ is established to simulate the temporal and spatial evolution of the coal and gas outburst, to obtain the stress transfer, gas migration, energy release, and damage zone development in the dynamic system during the outburst process. The simulation block geometry is 65 m in length, 33 m in width, and 55 m in height. The roadway is excavated in the x direction, and the roadway cross-section is square with side length of 4 m. The strata from top to bottom are roof shale, coal seam, mudstone, limestone, and sandstone. There is a fault fracture zone with width of 1.2 m. The geometric modeling is divided into free tetrahedron meshes. The complete mesh consists of 41,571 domain elements, 9295 boundary elements, and 1432 edge elements.

Figure 4c shows a section of the model under different excavation steps. The roadway initially advances along the horizontal x direction. When advanced 15 m, the direction of advance is changed to 20° inclined upward to expose the coal seam. When the advancing face is ~ 5 m separated from the footwall coal seam of the reverse fault, the coal and gas outburst occurs. The simulation of the roadway excavation is divided into four steps, and the advancing excavation distance is from 5 to 10 to 20 and then to 30 m, respectively. The reference line A-B-C-D-E–F in the center of the coal seam is set to monitor changes in the relevant parameters.

The vertical load of 15.3 MPa is applied from the overlying strata to the top boundary of the prismatic solution block in the z direction, and the horizontal load of 18.8 MPa and

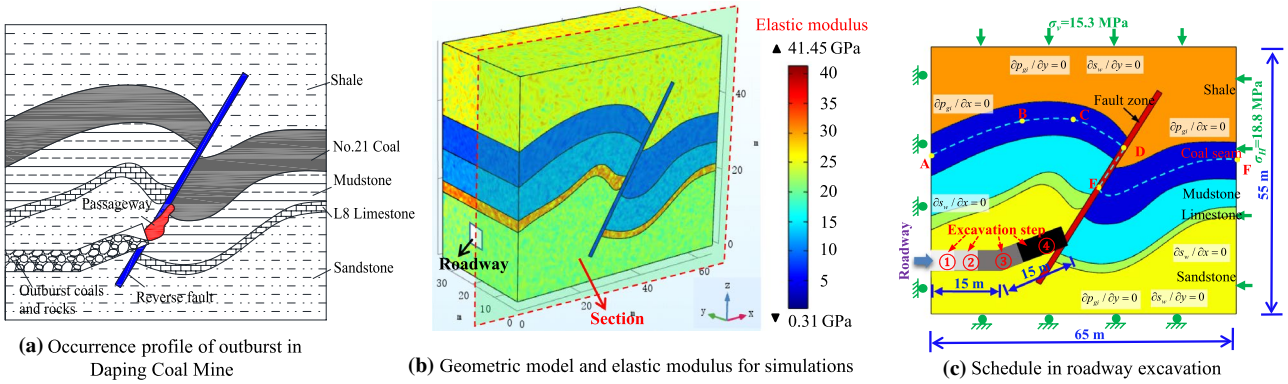

(a) Occurrence profile of outburst in Daping Coal Mine

(b) Geometric model and elastic modulus for simulations

(c) Schedule in roadway excavation

Fig. 4 Geometric model for simulations of spatio-temporal evolution of coal and gas outburst in Daping Coal Mine

12.8 MPa are applied on boundaries in the x and y directions with the bottom boundary set as fixed. The surrounding boundaries are impermeable. The initial gas pressure is 2.04 MPa, the coal permeability is 2.27×10^{-17} m^2, the water saturation in the fracture is 0.35, and the compressive strength of coal seam is 2.143 MPa. The mechanical properties of the microscopic REV of the coal–rock mass are heterogeneous in space. Assuming that the coal–rock mechanical parameters on the REVs obey a Weibull distribution, the initial values are randomly generated by the Monte Carlo method. The spatial distribution of elastic modulus of coal–rock mass is shown in Fig. 4b. The relevant parameters used in the simulation are shown in Table 1 and Table 2. Most of parameters were measured from experimental test on samples taken from the same coal seam in Daping Coal

Table 1 Relevant parameters for simulation of the evolution of outbursts in the dynamic system

Parameter name	Value	Parameter name	Value
Initial gas pressure (p_0, MPa)	2.04	Geothermal temperature (T_0, K)	300
Volume constant (V_L, m^3/kg)	0.0256	Maximum sorption induced strain (ε_{max})	0.0128
Pressure constant (P_L, MPa)	2.07	Molar mass of gas (M_g, g/mol)	16
Gas dynamic viscosity (μ_g, Pa·s)	1.84×10^{-5}	Molar gas constant (R, J/(mol·K)	8.314
Gas viscosity (μ_w, Pa·s)	1.03×10^{-3}	Benchmark temperature (T_s, K)	273.5
Initial water saturation (s_{wi})	0.35	Standard pressure (p_s, kPa)	101
Irreducible water saturation (s_{wr})	0.32	Expansion coefficient (f_m)	0.5
Porosity in rock (φ_{f10})	2.21	Increasing coefficient of permeability (α_D)	12
Gas desorption time (τ, d)	6	Increasing coefficient of gas desorption (α_{D1})	0.05
Initial porosity in coal (φ_{m0})	0.065	Porosity in fault (φ_{f20})	0.2
Initial fracture in coal (φ_{f0})	0.012	Rock density (ρ_r, kg/m^3)	2500
process coefficient (n)	1.25	Coal density (ρ_c, kg/m^3)	1470
slippage factor (b_k, MPa)	0.76	capillary pressure (p_{cgw}, MPa)	0.05

Table 2 Mechanical and transport parameters of the coal and rock mass

Parameter	Shale	Coal	Mudstone	Limestone	Sandstone	Fault fractured zone
Compressive strength (σ_c, MPa)	8.93	1.34	2.06	12.61	6.03	1.13
Tensile strength (σ_t, MPa)	2.16	0.48	0.68	2.624	1.16	0.32
Elastic modulus (E, GPa)	18.34	4.34	10.93	35.34	16.05	1.84
Degree of uniformity (m)	8	6	8	12	10	4
Poisson ratio (ν)	0.3	0.35	0.3	0.25	0.28	0.38
Initial permeability (k_0, 10^{-18}m^2)	0.57	22.7	1.27	1.25	85.7	8.21
Angle of internal friction (θ, °)	25.96	12.7	20.24	30.73	23.1	9.57

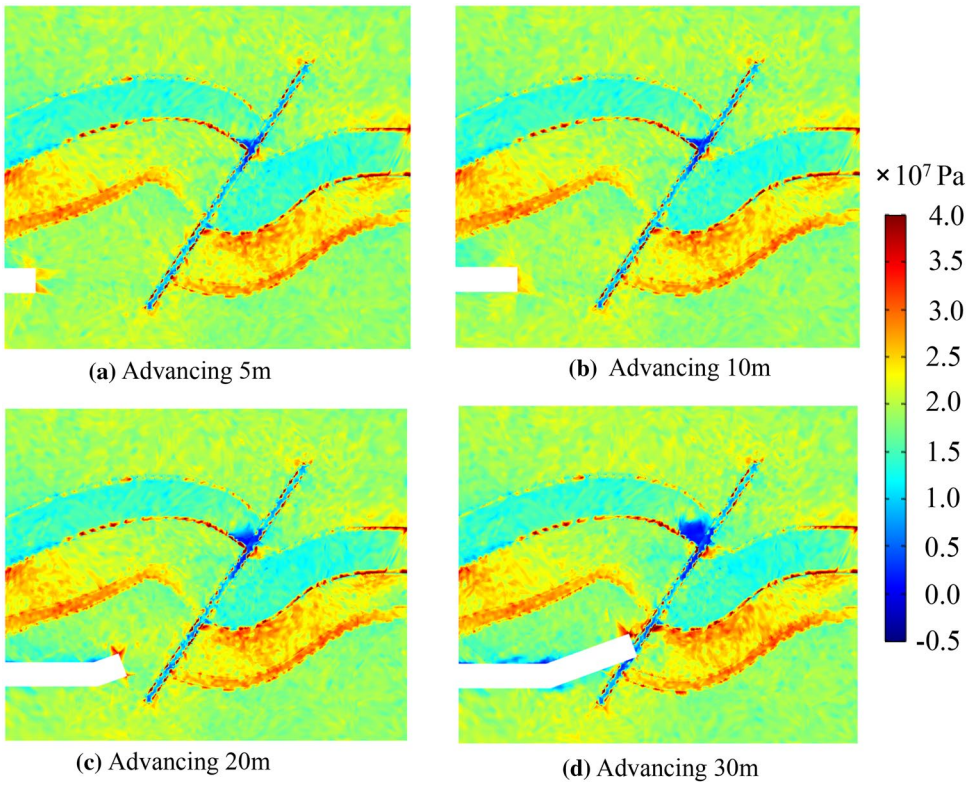

Fig. 5 Maximum principal stress within coal–rock mass during roadway excavation

Mine, while some of these parameters were cited from other literatures.

5.2 Stress Transfer and Damage Evolution During the Formation of the Outburst

The distribution of the maximum principal stress in the coal–rock mass after different advance lengths of excavation is shown in Fig. 5. When the roadway is excavated for 5 m, the stress increases ~ 2–4 m ahead of the roadway. The advancing face of the roadway remains distant from the fault, and the damage zone near the fault is small, indicating that the excavation has little effect on the fault damage zone. As the excavation of the roadway continues, the rock surrounding the roadway is damaged, and a stress-relief zone is generated in the floor and roof. With advance of the roadway, the stress-relief zone expands. The closer to the fault damage zone, the greater the impact of the roadway excavation on the failure of coal and rock near the fault. When the advancing face is excavated to 30 m, significant damage occurs at the intersection of the fault and the upper coal seam, and the stress in the coal–rock mass decreases rapidly.

The spatial distribution of damage in coal–rock mass for different advance lengths of the roadway excavation is shown in Fig. 6. The total damage zone can be divided into the damage zone around the roadway and the damage zone in fault region. When the roadway is excavated to 30 m, the advancing face is then close to the fault. The damage zone around the roadway and in the fault region are superimposed and connected. The coal–rock mass in the damage zone satisfies the formation criterion F_1 of the dynamic system, thus a coal and gas outburst initiates.

5.3 Evolution of Stress, Gas, and Energy During the Gas Outburst Instability

5.3.1 (1) Stress Transfer

When the instability criterion F_2 is satisfied, the failed coal–rock mass is ejected into the roadway and accompanied by a massive release of gas, resulting in a coal and gas outburst. In Fig. 7, the zone of reduction of the maximum principal stress in the coal–rock mass expands as the outburst time increases. When the outburst lasts 30 s, the zone of stress reduction is mainly distributed in the coal seam in the upper stratum, the reverse fault, and the rock surrounding the roadway. With an increase of the time of the outburst, the coal–rock mass above the advancing face is damaged and the stress is relieved. At 60 s, a zone of reduced stress appears and begins to expand in the coal seam in lower part of the

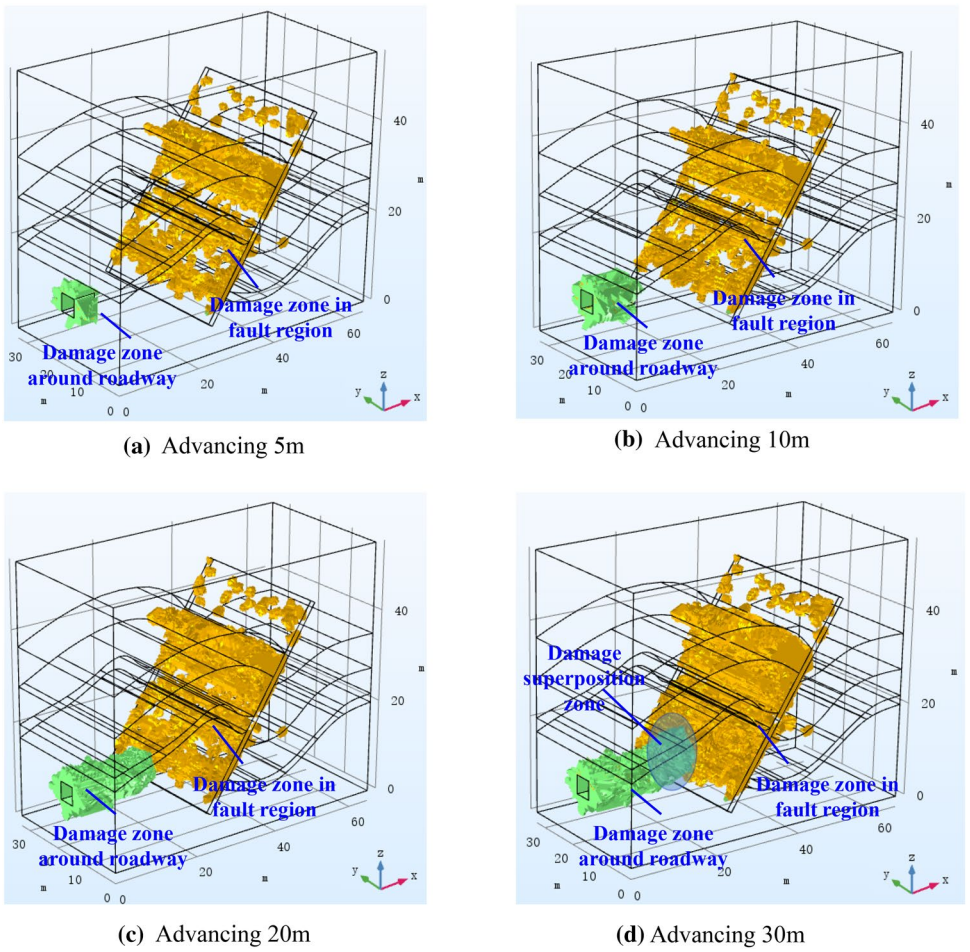

Fig. 6 Distribution of damage zone within the coal and rock mass during roadway excavation

(a) Advancing 5m

(b) Advancing 10m

(c) Advancing 20m

(d) Advancing 30m

fault. This zone reaches a maximum size when the outburst lasts for 180 s.

The stress distribution near the fault is complex. The zone of stress reduction in the coal–rock mass near the fault enlarges with time. The stress in the stress-relief area is then borne by the surrounding rock, leading to a stress increase in the coal–rock mass outside the red-stressed region. For point B, distant from the reverse fault, the ground stress is less affected in the outburst process. While for point C, near the fault, the stress field is strongly affected. The maximum principal stress reaches 17.73 MPa when the outburst has lasted 30 s. However, as the outburst continues, the stress is rapidly released and finally reduces to 1.7 MPa. The coal–rock mass at point C is initially intact. In the outburst process, damage occurs at point C, and the load-bearing ability decreases. The coal–rock mass at point D, located at the intersection of the upper coal seam and the fault, is damaged in the early stage of the outburst. As the outburst proceeds, damage increases, and the stress decreases from 2.83 MPa at 30 s to 1.08 MPa at 180 s.

5.3.2 (2) Gas Migration

The participation of gas is one of the main differences between coal and gas outburst and other dynamic disasters. In the coal seam, gas is mainly in the adsorbed state, accounting for more than 90% of the total gas. When the coal mass is damaged, the fracture space in the coal mass increases, and the state of equilibrium sorption is disrupted. The adsorbed gas desorbs and migrates to the fractures, and then participates in the process of the coal and gas outburst, providing a steady energy source for the outburst. When the high-pressure gas is rapidly depressurized, a volume expansion occurs and works on the coal–rock mass, which promotes the extension of fractures and fragments the coal (Zhao et al. 2016; Guo et al. 2016b).

The distribution of gas pressure in the fractures within the coal–rock mass is shown in Fig. 8. In the first 60 s of the outburst, the gas pressure slowly decreases, mainly in the zone located in the front of the roadway and the lower part of the fault. The fault damage zone is not connected at this time, as well as the high permeability zone. After 60 s, the damage zone propagates and the gas rapidly migrates to

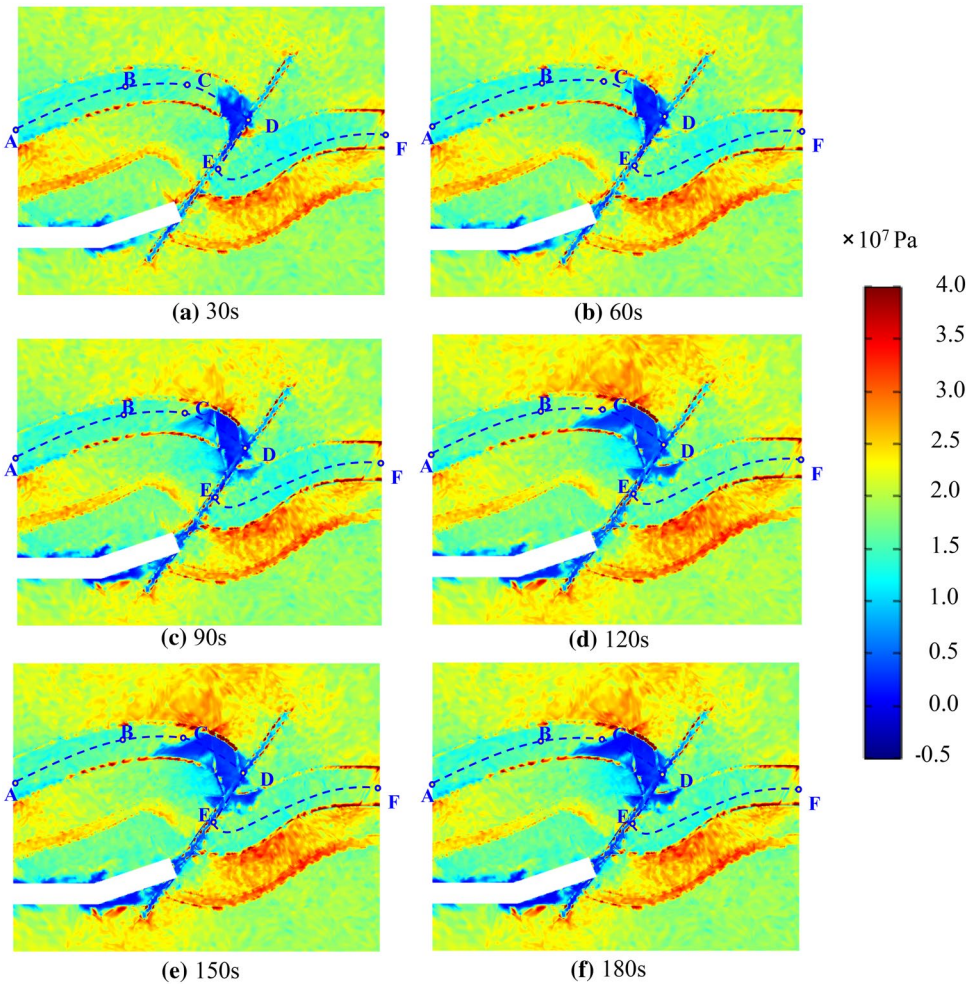

Fig. 7 Distribution of maximum principal stress in the coal and rock mass during outburst

the free space of the roadway, driven by the high pressure gradient and high permeability, resulting in a sharp drop in the gas pressure. In the coal seam close to the fault zone, the gas pressure rapidly decreases with time. The closer to the fault, the larger the decrease in gas pressure. In 60 s–150 s, the gas pressure decreases at a high rate, indicating that the gas outburst is severe over this time interval.

The fracture gas pressure at points B, C, and D is 1.95 MPa, 1.89 MPa, and 1.80 MPa, respectively, at 30 s, thus relatively uniform. When the outburst lasts for 180 s, the gas pressures at points B, C, and D are 1.57 MPa, 0.52 MPa, and 0.48 MPa, respectively. These are 21.9%, 74.1%, and 76.1% lower than the initial pressure of 2.04 MPa.

The distribution of gas pressure in the coal matrix is shown in Fig. 9. Compared with the fracture gas pressure, the rate of reduction in the matrix gas pressure is significantly slowed and the size of the zone of reduced pressure is clearly reduced. The reason may be that the gas diffusion rate in the matrix is slower than the gas seepage rate in the fracture. In the early stage of the outburst, the matrix gas pressure decreases slowly, and the zone of reduced pressure is mainly located ahead of the roadway and the lower part of the fault. With a decrease in the gas pressure in the fracture, the gas desorbs from the matrix, migrates to the fracture, and then rapidly migrates to the free space of roadway. The matrix gas pressure changes only slightly at 150 s and 180 s, indicating that the gas desorption is slow and the amount of outburst gas sharply reduces. At points C and D near the fault, the matrix gas pressure decreases rapidly, while at point B, far from the fault, it remains essentially unchanged. At 180 s, the matrix gas pressure at points B, C, and D is 2.03 MPa, 1.17 MPa, and 0.63 MPa respectively, which is 0.5%, 42.65%, and 68.78% lower than the initial pressure. The matrix gas pressure decreases more significantly in the area closer to the fault.

5.3.3 (3) Energy Dissipation

The coal and gas outburst process involves energy accumulation, release, and transformation. In the outburst, the accumulation of elastic potential energy and gas internal energy

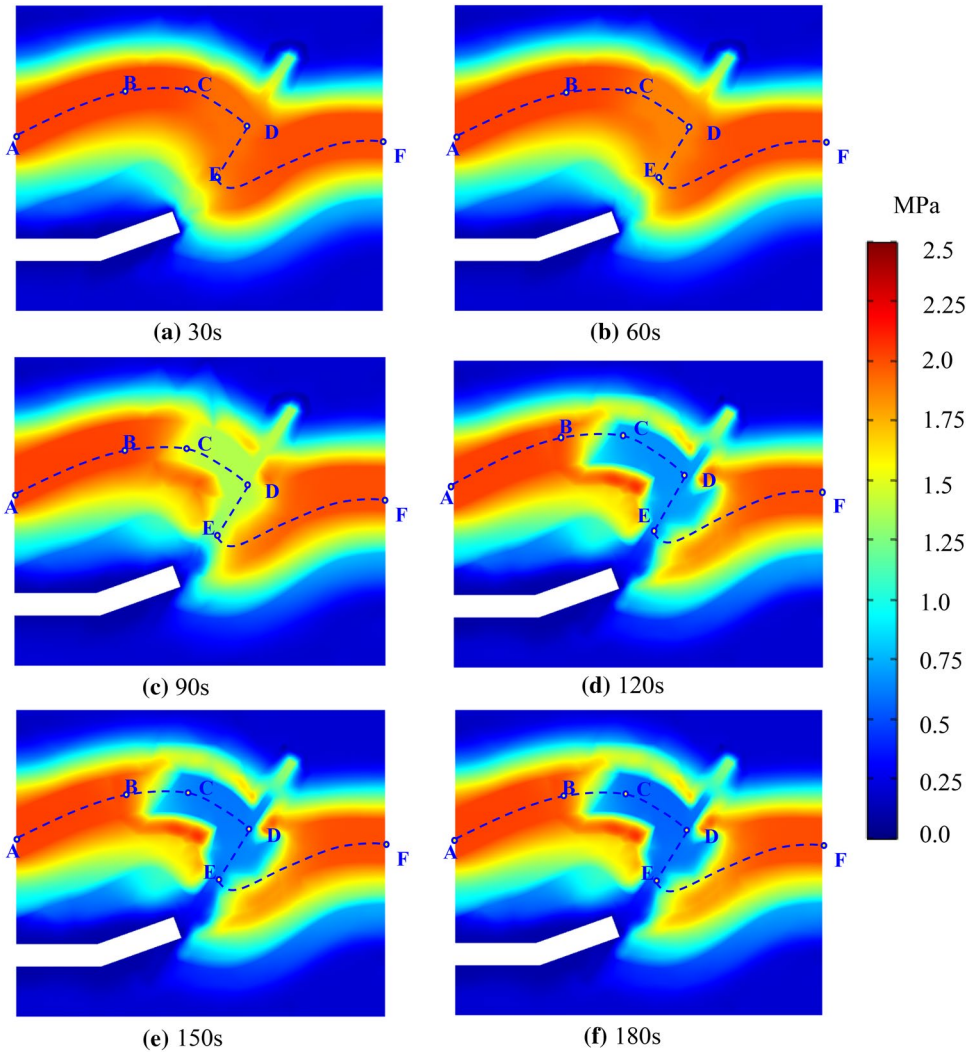

Fig. 8 Gas pressure distribution in fractures within the coal and rock mass during outburst

is continuously released and converted into comminution work and the kinetic energy of the high-speed motion of the coal–rock. The gas desorption speed slows until the release and the dissipation of energy in the dynamic system reaches a new equilibrium (Wang et al. 2013, 2015c).

The dissipated energy (E_d) in the outburst is mainly composed of the comminution/crushing work (E_f) in producing coal–rock fragments and the kinetic energy (E_k) for coal–rock ejection. Figure 10 shows the dissipated energy density of coal–rock mass in the damage zone. In the dynamic system, the position where the dissipated energy density is greater than 30 MJ/m^3 indicates that the energy density required to crush and eject the coal mass is significant. As time increases, the damage zone expands, the firmness coefficient in this zone decreases, caused by the increased damage. According to Eq. (6), the dissipated energy required to crush the coal–rock is greatly reduced. At 30 s, the dissipated energy density in most zones is greater than 30 MJ/m^3, except for the zone near the fault. As the zone of damage expands, the crushing work required for the damaged coal–rock mass decreases and the zone of the decreasing required energy density extends.

In the outburst, the energy released from the gassy coal–rock mass (E_s) includes the gravitational potential energy (E_p), the solid elastic energy (E_e), and the gas internal energy (E_g). Figure 11 shows the change of energy released from the gassy coal–rock mass in the damage zone during the outburst. At 30 s, the energy density that can be released from the coal–rock mass is limited. With the increase of time, the damage zone in coal mass expands, and gas desorption from the crushed coal accelerates. The adsorbed gas is quickly desorbed as free gas and accompanied by the

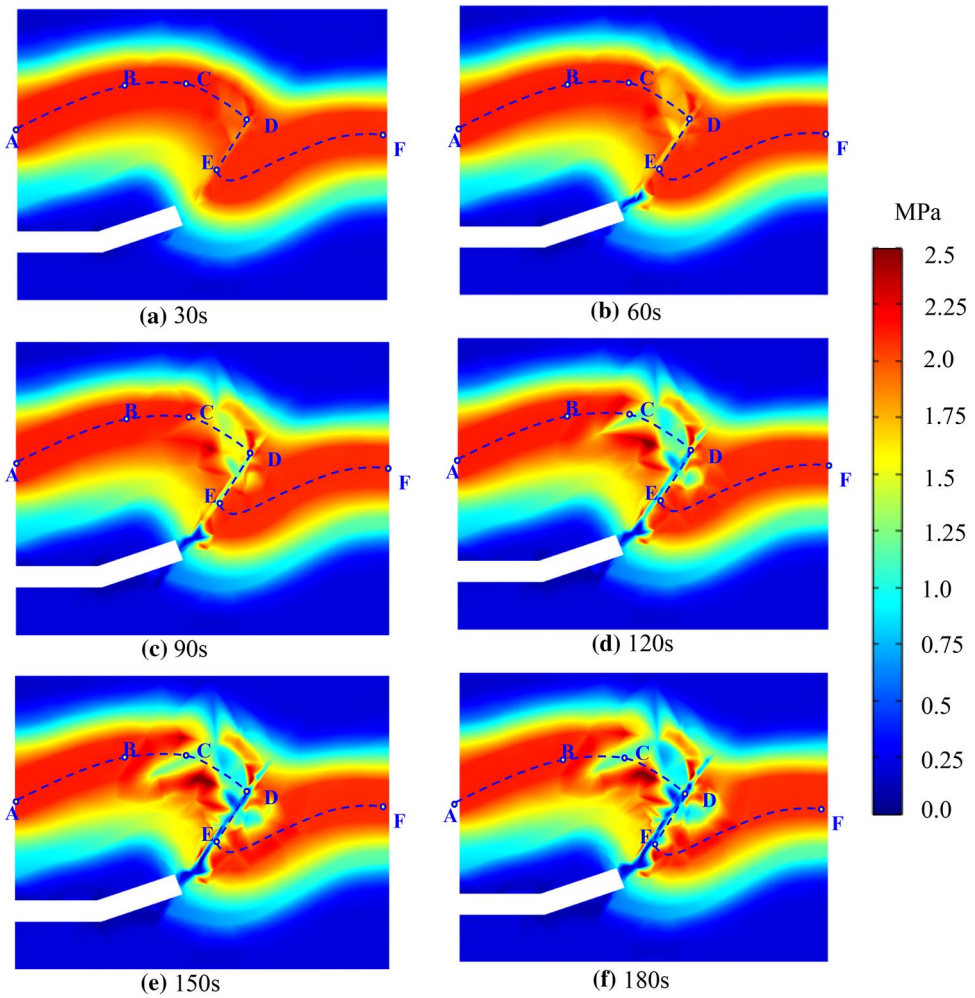

Fig. 9 Distribution of gas pressure in the coal matrix during outburst

release of internal gas energy. The gas pressure produces a tensile stress within the coal mass, comminutes the coal into small fragments, accelerates the process of coal damage and failure, and finally the high-pressure gas ejects the coal mass into the roadway. In Fig. 11, the released energy density in the damage zone increases with time, and this zone expands. The maximum released energy density can reach 25 MJ/m^3 in the coal seam near the fault. As time continues, the released energy density near the fault increases. In 0–60 s, the increasing rate of the released energy density is slow. After 60 s, the gas internal energy is released rapidly, and the released energy density increases sharply. Gas internal energy density dominates the change of released energy density, and thus the trends in the released energy density and the adsorbed gas are opposite.

Figure 12 shows the variation in the released energy density with time for the reference points. At point B, the required dissipated energy density is maintained at 116 MJ/m^3, while the energy released from the coal mass is only 0.58 MJ/m^3-far less than the energy required for instability. According to the instability criterion F_2, the coal mass will be stable, and an outburst will not occur. At point C, the required dissipated energy is higher at first, and results in damage to the coal mass and a reduction in the firmness coefficient of the coal mass, resulting in the reduction of the required dissipated energy and thus instability of dynamic system. At 120 s, the dissipated energy at point C is 1.77 MJ/m^3, and the released energy is 8.85 MJ/m^3. Clearly, the instability criterion F_2 is satisfied to trigger an outburst. At point D, the required dissipated energy density is initially low, at 1.96 MJ/m^3. With the rapid release in desorbed gas, the energy density released at this point reaches 2.19 MJ/m^3 at 90 s, which is greater than the required dissipated energy density, satisfying the instability criterion F_2, and ultimately an outburst occurs.

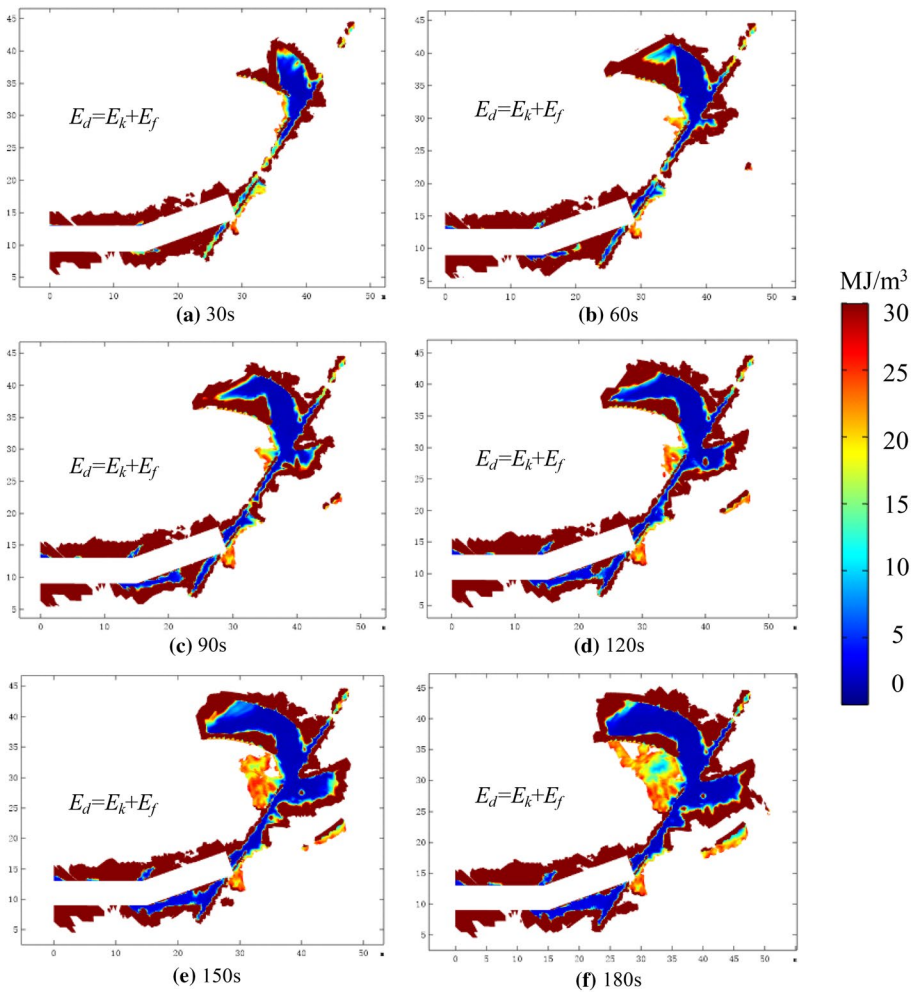

Fig. 10 Distribution of dissipated energy density within coal and rock mass in the area of damage during outburst

5.4 Spatial–Temporal Evolution of the Outburst Dynamic System

The coal–rock mass with the largest changes in the geo-stress, gas pressure, and mechanical properties are the main places where outburst occurs. Due to the low permeability in the original intact coal–rock mass, gas outflow and pressure dissipation are difficult and cannot participate in the dynamic process of gas outburst. In general, the changes of gas pressure, geo-stress, and energy in the undamaged coal–rock mass are small, while these parameters in the damaged zone all change significantly. We define the spatial scale of the outburst dynamic system as the damaged zone of the coal–rock mass, satisfying the formation criterion F_1.

Compared with the damage to the coal–rock, the instability is a phenomenon where the coal–rock mass is broken and loses its load-bearing capacity under the applied stress. One of the main characteristics of coal and gas outbursts is that the gassy coal–rock mass in a certain zone suddenly loses its load-bearing capacity. Therefore, an instability criterion is a basic requirement for the occurrence of coal and gas outbursts. Accordingly, the occurrence of coal and gas outbursts depends on the released energy density–that it is greater than the required dissipated energy density, which satisfies the energy-based instability criterion F_2 of the dynamic system. The newly outburst-prone coal–rock mass needs to reach the instability criterion F_2 after the formation criterion F_1. Here, we define the spatial scale of the outburst geological body as the coal–rock mass satisfying both criteria F_1 and F_2. Thus, the spatial scale of the outburst determines the size, spatial position, and shape of the outburst cavity. It characterizes the intensity of the outburst and is the key area in which to prevent an outburst.

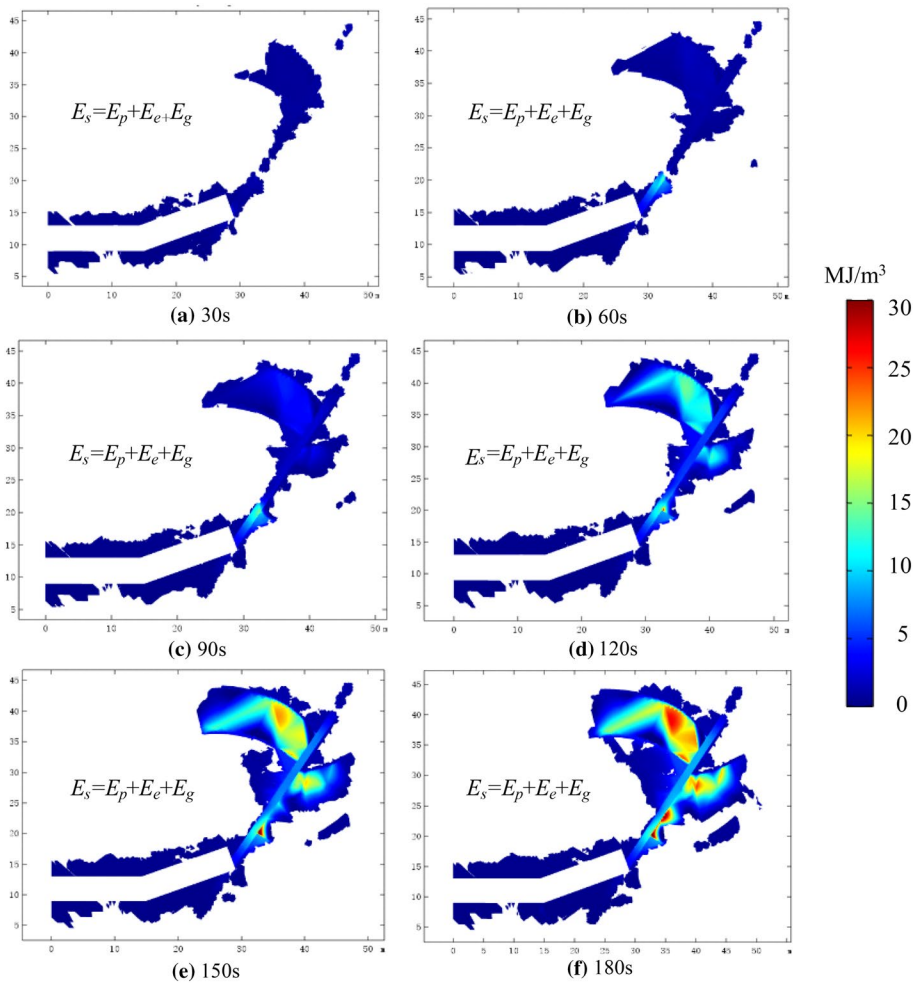

Fig. 11 Distribution of energy density released by gas-bearing coal and rock mass during outburst

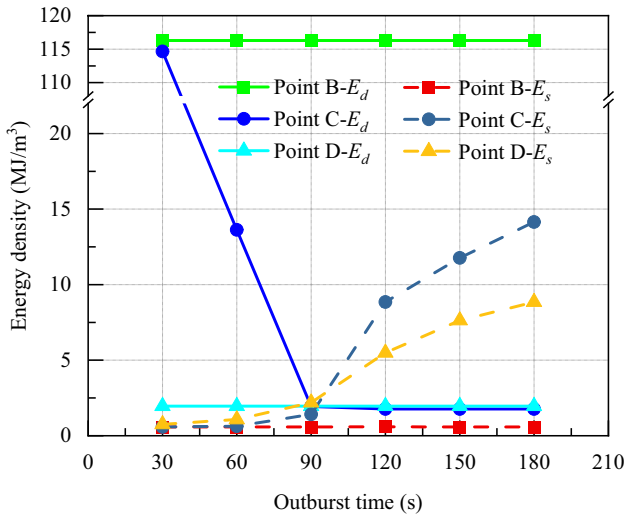

Fig. 12 Variation of energy density released by coal and rock mass during outburst

In this work, the dynamic system and the geological body of coal and gas outburst are constructed for the outburst accident in the Daping Coal Mine. The spatial scale of the dynamic system and the geological host to the outbursts are given. The volumes of coal–rock, coal mass, and rock mass are calculated, as shown in Figs. 13–16. When the outburst occurs for 60, 90, 120, and 180 s, the total volume of coal and rock in the outburst dynamic system is 4766, 5230, 5699, and 6779 m^3, respectively. The total volume of coal–rock in the outburst geological body is 96, 926, 1572, and 1698 m^3, respectively.

In Fig. 13, when the outburst occurs for 60 s, the volume satisfying the instability criterion F_2 is small. The fault damage zone is not effectively connected, and the gas in the coal seam fails to participate in the process of outburst. At this duration, the volume of the outburst in the geological body only accounts for 2.01% of the geo-dynamic system.

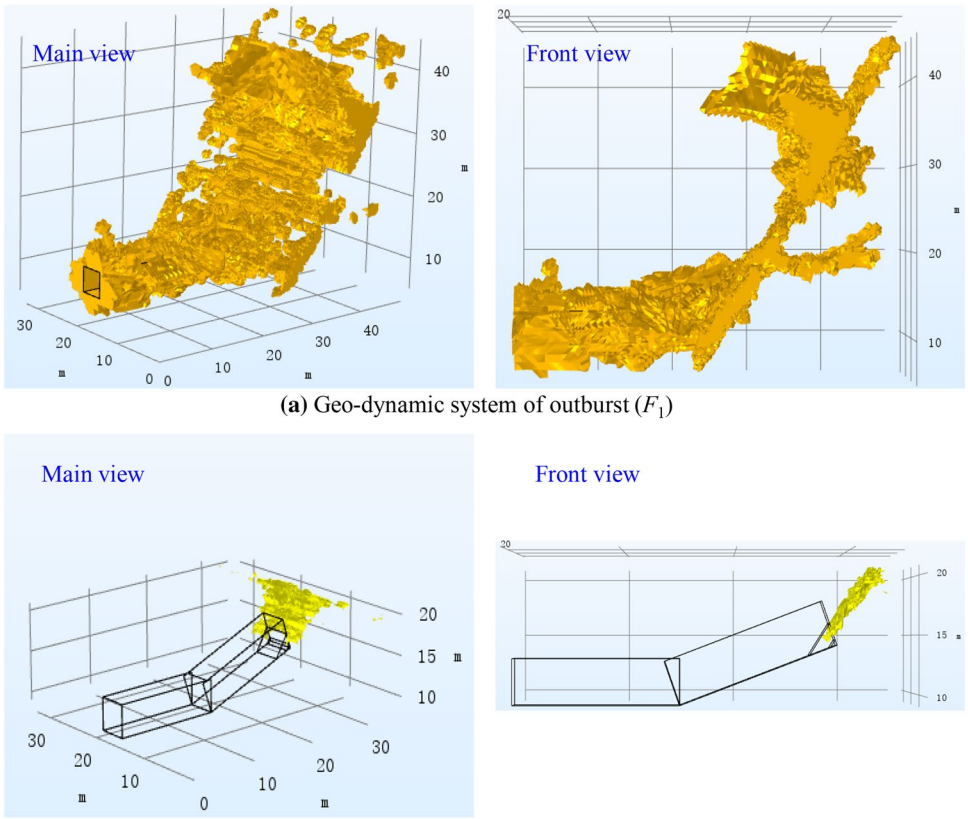

Fig. 13 Spatial scale for dynamic system and geological body of outburst at 60 s

(a) Geo-dynamic system of outburst (F_1)

(b) Geological body of outburst (F_1 and F_2)

In Fig. 14, when the outburst occurs for 90 s, the fault damage zone has been effectively connected, and the desorbed gas can release energy, promote instability of the dynamic system, and rapidly extend the outburst through the geological body. At this duration, the outburst geological body only accounts for 17.7% of the geo-dynamic system.

In Fig. 15, the outburst has occurred for 120 s, and the outburst geological body expands by 646 m^3, accounting for 27.6% of the geo-dynamic system. The outburst is still severe during this period, with a large amount of gas releasing energy and participating in the outburst process.

In Fig. 16, the outburst has occurred for 180 s, the outburst geological body expands by 126 m^3, and the outburst geological body accounts for 25.1% of the geo-dynamic system. The outburst intensity tends to stabilize during this period, and the outburst terminates.

In Fig. 17a, the spatial scale of the geo-dynamic system satisfying the formation criterion F_1 increases with the outburst time, from 3816 m^3 at 30 s to 6779 m^3 at 180 s. The volume of rock mass in the geo-dynamic system is much larger than that of coal mass, due to the damage to the rock surrounding the roadway in the outburst geo-dynamic system. In Fig. 17b, the volume of the outburst in the geological body satisfying both the formation criterion F_1 and the instability criterion F_2 shows a slow–rapid–slow trend with time. From 60 to 120 s, the outburst geological body enlarges most significantly. During this period, the outburst intensity is the largest, which is the most serious stage in the disaster. In general, the volume of coal in the outburst geological body is greater than that of rock. At 180 s, the outburst is essentially terminated and the outburst volume of total coal–rock, coal, and rock is 1698 m^3, 1154 m^3, and 544 m^3, respectively. According to the on-site outburst in the Daping Coal Mine, the volume of the outburst coal–rock is 1461 m^3, amounting for 1894 t of coal–rock, 1362 t of coal, and 532 t of rock. By comparison, the volume of the geological body obtained in the simulation is close to that of on-site outburst, with an error of ~ 16.2%. The reason for this slight mismatch may be the strong heterogeneity of the mechanical properties of the coal–rock and the difficulty in obtaining accurate parameter for the coal–rock masses in the outburst cavity.

Figure 18 shows the volume ratio of the outburst geological body to the geo-dynamic system. Before the outburst occurs

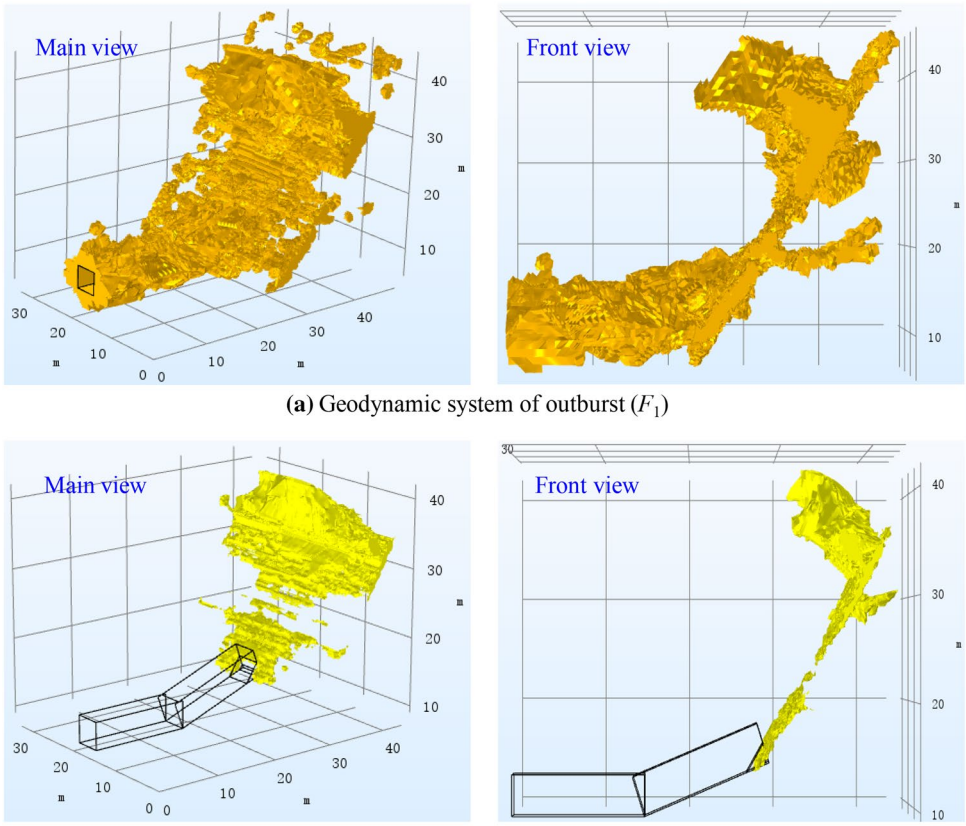

Fig. 14 Spatial scale for dynamic system and geological body of outburst at 90 s

(a) Geodynamic system of outburst (F_1)

(b) Geological body of outburst (F_1 and F_2)

120 s, the volume ratio increases with the outburst time, and reaches a maximum value of 27.58% at 120 s. After that, the volume ratio gradually decreases. The total amount of outburst of the geological body only accounts for approximately a quarter of that of the outburst dynamic system. This indicates that there is a large volume of coal–rock mass that provides motive power and energy for the outburst of coal–rocks in the dynamic system. This coal–rock mass has contributed to the outburst disaster, although has not been ejected.

6 Preventative Countermeasures for Coal and Gas Outbursts

We observe that the final outburst volume closely approximates the volume of the coal–rock zone satisfying the instability criterion F_2. This implies that the energy accumulation and release in the dynamic system dominate the initiation and development of outburst. The change in energy comprehensively reflects the mechanical strength of coal–rock mass, the geo-stress state, and the gas ad-desorption. In the initialization of the outburst, the fractures extend when the coal mass is destroyed or crushed under the combined action of gas pressure and external loading. This process consumes the major energy to increase the surface energy of coal–rock fragments. An increase in coal–rock strength will increase the crushing work required, and as a result, the energy threshold required for an outburst will also be increased. On the contrary, an increase in gas pressure and geo-stress will increase the energy accumulated in the gassy coal–rock mass, and thus the potential energy released by the outburst will be increased. From the results of the simulation, the formation of the dynamic system is a prerequisite for the release of potential energy, while a released energy density greater than the required dissipation of energy density is the key to determine whether the outburst can continue.

In Fig. 19, the effective stress, dominated by geo-stress, acts on the coal–rock mass. When the formation criterion F_1 of the dynamic system is satisfied, damage occurs to form the outburst. When the coal–rock mass has low strength, the

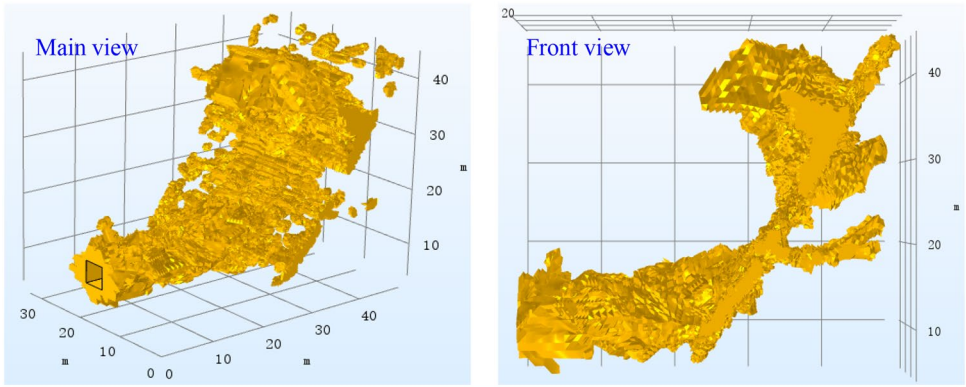

(a) Geodynamic system of outburst (F_1)

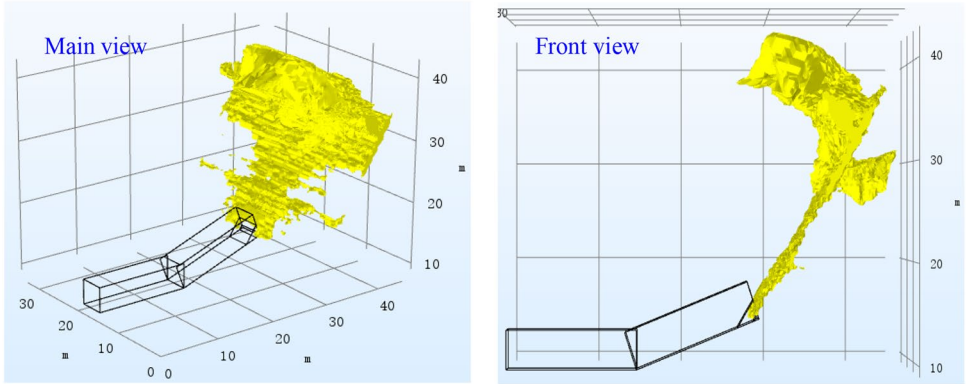

(b) Geological body of outburst (F_1 and F_2)

Fig. 15 Spatial scale for geo-dynamic system and geological body of outburst at 120 s

system meets the instability criterion F_2 under the action of geo-stress and gas pressure alone and instability as an outburst occurs. Therefore, preventative countermeasures may be proposed to eliminate the risk of outbursts by controlling the major factors impacting the formation criterion F_1 and instability criterion F_2 of the dynamic system.

The high geo-stress in the coal seam formed by the mining stress and tectonic stress are the major controlling factors influencing the formation criterion F_1 for the dynamic system. This dominates the mechanical damage and failure process, and reduces the strength of the coal–rock mass. Fractures and pores within the coal–rock mass under the high stress state are often compacted and closed, which seals gas migration. In engineering practice, the regional measures of using a mining protective layer and local measures of hydraulic punching or large diameter relief boreholes are usually adopted to alleviate the high geo-stress, namely the "unloading" countermeasure. In this situation, the spatial scale of the outburst-prone dynamic system cannot be formed, and the risk of coal and gas outburst is reduced or eliminated.

However, if the outburst geo-dynamic system is formed, an outburst disaster can also be prevented by addressing the instability criterion F_2 of the geo-dynamic system. The regional measures of pre-drainage of coal seam gas and the local measures of gas drainage ahead of the advancing roadway or mining face are usually adopted to reduce the gas pressure and content in the coal seam, namely the "depressurization" countermeasure. By this, the instability criterion F_2 is obviated and the likelihood of an outburst is avoided.

Therefore, the prevention of coal and gas outbursts based on the dynamic system includes countermeasures of "unloading" and "depressurization". "Unloading" is to reduce the geo-stress to improve the stress conditions of the coal seam, and to obviate the formation criterion F_1. "Depressurization" is to reduce the gas pressure and gas content in the coal seam, and to obviate instability criterion F_2. By applying one or all of these countermeasures, the coal–rock mass can maintain its stability, and thus eliminate the danger of an outburst.

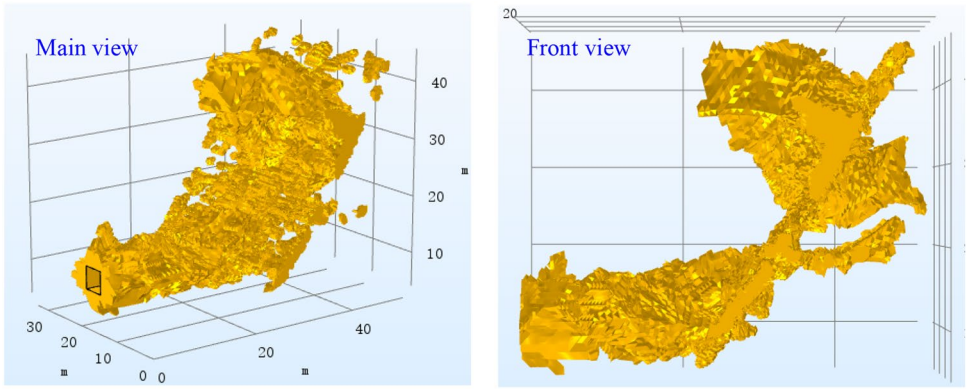

(a) Geodynamic system of outburst (F_1)

(b) Geological body of outburst (F_1 and F_2)

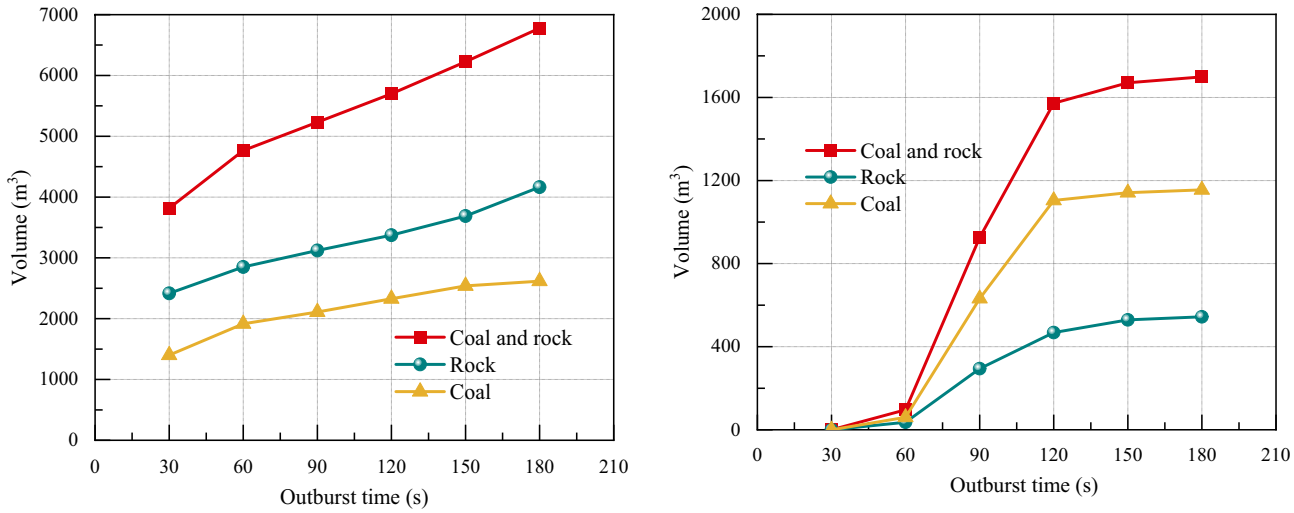

(a) The geo-dynamic system (criterion F_1)

(b) Geological body (criterion F_1+F_2)

Fig. 16 Spatial scale for dynamic system and geological body of outburst at 180 s

Fig. 17 Evolution of spatial scale for dynamic system and geological body of outburst with time. **a** The geo-dynamic system (criterion F_1), **b** Geological body (criterion F_1+F_2)

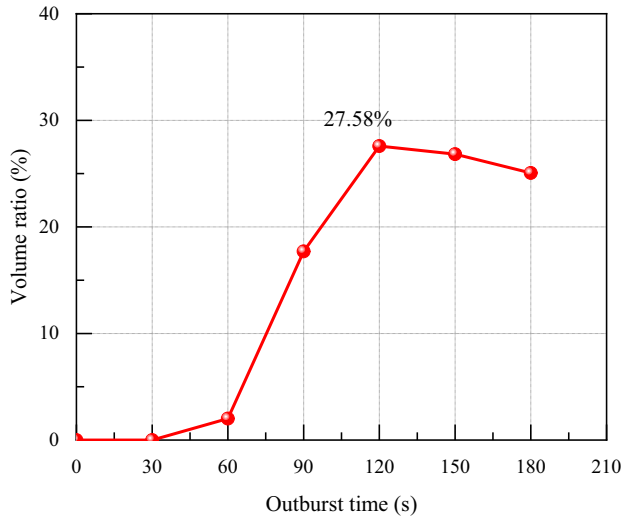

Fig. 18 Volume ratio of the outburst geological body to the dynamic system

7 Conclusion

(1) Mechanisms contributing to the evolution of coal and gas outbursts are explored as a dynamic system to reveal key controls on criteria for the formation and instability of such gas outbursts. The outburst progresses as a dynamic system in four stages—*initialization*, *formation*, *development* through *termination*.

(2) A stress–damage–seepage coupling model for outbursts in coal seams is established. This comprises governing equations defining the stress field and gas transport from desorption, then diffusion through the matrix to the embedded fractures. This model is used to simulate the macro-fracture propagation and gas migration contributing to coal and gas outbursts.

(3) The spatial–temporal evolution of coal and gas outburst is simulated using this model and the relative impacts of stress transfer, gas migration, energy accumulation and then release in the dynamic system revealed. The dynamic triggering of a coal and gas outburst occurs when the mining-induced damage zone is superimposed onto the tectonically induced damage zone ahead of the roadway.

(4) The spatial scales of the outburst dynamic system and the geological body are defined and provide the spatial basis for the implementation of outburst countermeasures. A three-dimensional view of the evolving dynamic system is recovered from these models with volumes in good agreement with the outbursts observed forensically on site.

(5) The formation of a dynamic system is a prerequisite for the release of the potential energy. A released energy density greater than the required dissipation energy density is the key feature to determine whether the outburst can continue. Thus, countermeasures for the prevention of coal and gas outbursts based on such a dynamic system include “unloading” and “depressurization”.

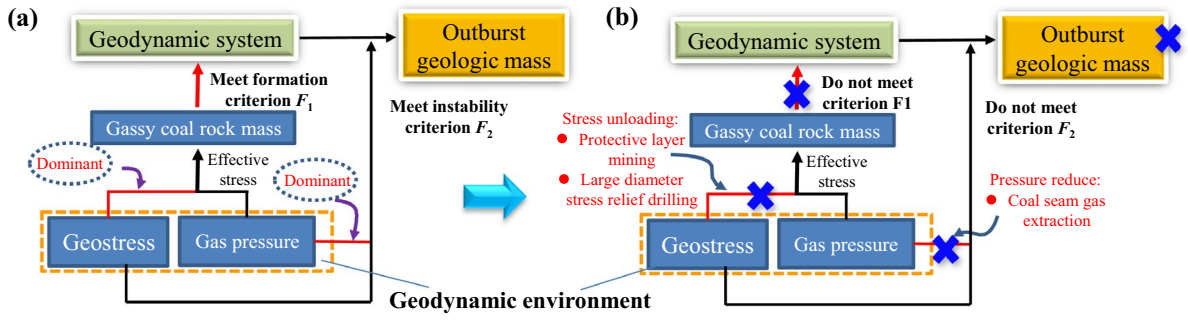

Fig. 19 Prevention countermeasures of coal and gas outburst based on the dynamic system

Acknowledgements This research was financially supported by the National Natural Science Foundation of China (Grant Nos. 52004117, 52174117 and 51674132), the Postdoctoral Science Foundation of China (Grant Nos. 2021T140290 and 2020M680975), the Discipline Innovation Team of Liaoning Technical University (Grant No. LNTU20TD-03), and the Natural Science Foundation of Liaoning Province (Grant No. 2020-KF-13-05). Derek Elsworth acknowledges support from the G. Albert Shoemaker endowment.

Funding This study was funded by National Natural Science Foundation of China, 52004117, Chaojun Fan,52174117, Chaojun Fan,51674132, Chaojun Fan, Postdoctoral Science Foundation of China, 2021T140290,Chaojun Fan, 2020M680975, Chaojun Fan, Discipline Innovation Team of Liaoning Technical University, LNTU20TD-03, Sheng Li,Natural Science Foundation of Liaoning Province, 2020-KF-13-05, Chaojun Fan,G. Albert Shoemaker endowment.

Data Availablity The data that support the findings of this study are available from the corresponding authors upon reasonable request.

References

An F, Cheng Y, Wang L et al (2013) A numerical model for outburst including the effect of adsorbed gas on coal deformation and mechanical properties. Comput Geotech 54:222–231

Chen S, Wei C, Yang T et al (2018) Three-dimensional numerical investigation of coupled flow-stress-damage failure process in heterogeneous poroelastic rocks. Energies 11(8):1923

Cui X, Bustin RM (2005) Volumetric strain associated with methane desorption and its impact on coalbed gas production from deep coal seams. AAPG Bull 89(9):1181–1202

Fan C, Li S, Luo M et al (2017) Coal and gas outburst dynamic system. Int J Min Sci Technol 27(1):49–55

Fan C, Elsworth D, Li S et al (2019) Thermo-hydro-mechanical-chemical couplings controlling CH4 production and CO2 sequestration in enhanced coalbed methane recovery. Energy 173:1054–1077

Guo H (2017) Equivalent characteristics of coal with dual pore structure and its influence mechanism on its mechanical and osmotic properties [D]. China University of Mining and Technology, Xuzhou

Guo X, Ma N, Zhao X et al (2016a) General shapes and criterion for surrounding rock mass plastic zone of round roadway. J China Coal Soc 41(8):1871–1877

Guo H, Cheng Y, Ren T et al (2016b) Pulverization characteristics of coal from a strong outburst-prone coal seam and their impact on gas desorption and diffusion properties. J Nat Gas Sci Eng 33:867–878

Guo H, Yu Y, Wang K et al (2023) Kinetic characteristics of desorption and diffusion in raw coal and tectonic coal and their influence on coal and gas outburst. Fuel 343:127883

Hu S (2015) Research on the solid coupling behavior and mechanism of multiscale fissure coal gas [D]. China University of Mining and Technology, Xuzhou

Hu Q, Zhou S, Zhou X (2008) Mechanical mechanism of coal and gas outburst process. J China Coal Soc 33(12):1368–1372

Kong X, He D, Liu X et al (2022) Strain characteristics and energy dissipation laws of gas-bearing coal during impact fracture process. Energy 242:123028

Li C, Xie B, Cao J et al (2012) The energy evaluation model of coal and gas outburst intensity. J China Coal Soc 37(09):1547–1552

Li S, Fan C, Han J et al (2016) A fully coupled thermal-hydraulic-mechanical model with two-phase flow for coalbed methane extraction. J Nat Gas Sci Eng 33:324–336

Li X, Xue H, Chen L et al (2021) Energy dissipation laws and hole safety dimensions of coal and gas outburst shock wave passing through door wall. J China Coal Soc 46(12):3934

Liang B (2000) Solid-current coupling instability theory of coal and gas outburst [M]. Geological Publishing House, Beijing, pp 32–38

Liu L, Li S, Xu G (2016) Gas seepage-stress-damage coupling model of mining coal rock. Safety Coal Min 4:15–19

Liu T, Lin B, Fu X et al (2021) Mechanical criterion for coal and gas outburst: a perspective from multiphysics coupling. Int J Coal Sci Technol 8:1423–1435

Lu D, Wang G, Du X et al (2017) A nonlinear dynamic uniaxial strength criterion that considers the ultimate dynamic strength of concrete. Int J Impact Eng 103:124–137

Lu D, Zhang Y, Zhou X et al (2023) A robust stress update algorithm for elastoplastic models without analytical derivation of the consistent tangent operator and loading/unloading estimation. Int J Numer Anal Meth Geomech 47(6):1022–1050

Luo M, Fan C, Li S et al (2018) Failure criteria of the geo-dynamic system of coal and gas outburst. J China Univ Min Technol 1:137–144

Ma Y, Nie B, He X et al (2020) Mechanism investigation on coal and gas outburst: an overview. Int J Miner Metall Mater 27:872–887

Pan Z, Connell L (2012) Modelling permeability for coal reservoirs: a review of analytical models and testing data. Int J Coal Geol 92:1–44

Rudakov D, Sobolev V (2019) A mathematical model of gas flow during coal outburst initiation. Int J Min Sci Technol 29(5):791–796

Shu L, Wang K, Qi Q (2017) key structural body theory of coal and gas outburst. Chin J Rock Mech Eng 36(02):347–356

Shu L, Wang K, Liu Z et al (2022) A novel physical model of coal and gas outbursts mechanism: insights into the process and initiation criterion of outbursts. Fuel 323:124305

Shu L, Yuan L, Li Q et al (2023) Response characteristics of gas pressure under simultaneous static and dynamic load: implication for coal and gas outburst mechanism. Int J Mining Sci Technol 33(2):155–171

Shu L, Yuan L, Li Q et al (2023b) Response characteristics of gas pressure under simultaneous static and dynamic load: implication for coal and gas outburst mechanism. Int J Min Sci Technol 33(2):155–171

Sobczyk J (2014) A comparison of the influence of adsorbed gasses on gas stresses leading to coal and gas outburst. Fuel 115:288–294

Soleimani F, Si G, Roshan H et al (2023) Numerical modelling of coal and gas outburst initiation using energy balance principles. Fuel 334:126687

Tang C, Rui Y, Liu H et al (2000) Numerical simulation of RFPA-2D with gas sample protrusion. J China Coal Soc 25(05):501–505

Tian X, Song D, He X et al (2021) Investigation on micro-surface adhesion of coals and implications for gas occurrence and coal and gas outburst mechanism. J Nat Gas Sci Eng 94:104115

Tu Q, Cheng Y, Xue S et al (2021) Energy-limiting factor for coal and gas outburst occurrence in intact coal seam. Int J Min Sci Technol 31(4):729–742

Wang C, Cheng Y (2023) Role of coal deformation energy in coal and gas outburst: a review. Fuel 332:126019

Wang S, Elsworth D, Liu J (2013) Permeability evolution during progressive deformation of intact coal and implications for instability in underground coal seams. Int J Rock Mech Min Sci 58:34–45

Wang G, Wu M, Cheng W et al (2015a) Analysis of energy conditions for coal and gas outburst and factors influencing outburst intensit. Rock Soil Mech 36(10):2974–2982

Wang G, Wu M, Wang H et al (2015b) Sensitivity analysis of factors affecting coal and gas outburst based on a energy equilibrium model. Chin J Rock Mech Eng 34(02):238–248

Wang S, Elsworth D, Liu J (2015c) Rapid decompression and desorption induced energetic failure in coal. J Rock Mech Geotech Eng 7(3):345–350

Wang H, Zhang B, Yuan L et al (2022) Analysis of precursor information for coal and gas outbursts induced by roadway tunneling: a simulation test study for the whole process. Tunn Undergr Space Technol 122:104349

Wu Y, Liu J, Elsworth D et al (2010) Development of anisotropic permeability during coalbed methane production. J Nat Gas Sci Eng 2(4):197–210

Xiong Y, Huang R, Luo J, et al. Theoretical analysis and experimental study of energy dissipation of coal and gas outburst[J]. Chinese Journal of Rock Mechanics and Engineering, (s2): 3694–3702

Xu T, Tang C, Yang T et al (2006) Numerical investigation of coal and gas outbursts in underground collieries. Int J Rock Mech Min Sci 43(06):905–919

Xu J, Yang X, Zhou B et al (2019) Study of evolution law of gas pressure and temperature in coal seam during outburst. J China Univ Min Technol 48(6):1177–1187

Xue Y, Gao F, Liu X (2015) Effect of damage evolution of coal on permeability variation and analysis of gas outburst hazard with coal mining. Nat Hazards 79(2):999–1013

Xue S, Tu Q, Hao Y et al (2023) Occurrence and development criteria of coal and gas outbursts based on energy conversion. Fuel 341:127781

Yuan L (2016) Control of coal and gas outbursts in Huainan mines in China: a review. J Rock Mech Geotech Eng 8(4):559–567

Zhang M, Xu Z, Pan Y et al (1991) Unified instability theory of burst and outburst. J Coal Sci 04:48–53

Zhang C, Xu J, Peng S et al (2018) Advances and prospects in physical simulation of coal and gas outburst. Coal Geol Explor 46(4):28–34

Zhang C, Wang E, Xu J et al (2021) A new method for coal and gas outburst prediction and prevention based on the fragmentation of ejected coal. Fuel 287:119493

Zhao W, Cheng Y, Jiang H et al (2016) Role of the rapid gas desorption of coal powders in the development stage of outbursts. J Nat Gas Sci Eng 28:491–501

Zheng C, Kizil M, Chen Z et al (2017) Effects of coal damage on permeability and gas drainage performance. Int J Min Sci Technol 27(5):783–786

Zhou A, Hu J, Gong W et al (2021a) The instability criticality and safety factor of coal-gas outburst induced by shear failure based on limit analysis. Fuel 303:121245

Zhou A, Zhang M, Wang K et al (2021b) Near-source characteristics of two-phase gas–solid outbursts in roadways. Int J Coal Sci Technol 8:685–696

Zhou X, Lu D, Zhang Y et al (2022) An open-source unconstrained stress updating algorithm for the modified Cam-clay model. Comput Methods Appl Mech Eng 390:114356